Hybrid Energy Harvesting in 3-D IC IoT Devices

Boris Vaisband and Eby G. Friedman

Department of Electrical and Computer Engineering
University of Rochester, Rochester, New York 14627 USA
[bvaisban,friedman]@ece.rochester.edu

***Abstract*— Three-dimensional integrated circuits are a natural platform for IoT devices. IoT devices exhibit a small footprint, integrate disparate technologies, and require long term sustainability (extremely low power or self powered). A hybrid energy harvesting system within a three-dimensional integrated circuit is proposed in this paper. The harvesting system exploits different types of energy available from the ambient (electromagnetic, solar, thermal, and kinetic). Integration of the hybrid harvesting system onto a three-dimensional platform ensures that each type of harvested energy can be individually optimized. In addition, lower parasitic impedances are exhibited within the three-dimensional structure, leading to improved efficiencies in the energy harvesting process. For an example IoT system, the power requirements are less than 57% of the power delivered to the load.**

I. Introduction

The Internet of Things (IoT) is a novel computing paradigm based on connecting physical devices to the global network. IoT devices should typically exhibit the following characteristics [1]: (1) small physical dimensions, (2) communication (typically wireless) capability, (3) sensing/actuation modality, and (4) low energy consumption. In addition to these key characteristics, IoT devices operate in extreme environments, such as automotive engines, industrial facilities, building automation, home appliances, and corrosive surroundings such as within or on the human body. IoT devices need to withstand hostile environments such as increased and highly variable temperatures, liquid immersion, and significant vibration.

Three-dimensional (3-D) integrated circuits (ICs) are a platform for heterogeneous integration, exhibiting a small form factor [2]. These traits of 3-D ICs make the 3-D platform a natural companion for IoT devices. The disparate technologies of IoT devices, including MEMS sensors and actuators, RF and wireless communication, energy harvesting circuitry, and computational logic, can be integrated as individual layers within a 3-D structure. Interface circuits should efficiently communicate information from the IoT sensors to the relevant layer(s) within a 3-D IC, and from the on-chip controllers within a 3-D system to the IoT actuators.

The layers within a 3-D IC are connected by through substrate vias (TSVs) [3]. The TSVs are short vertical interconnections (typically 20 μm in length and 2 to 4 μm in diameter [2]) that carry a variety of signals (power, clock, and data) between different layers within a 3-D IC.

This research is supported in part by the Binational Science Foundation under Grant No. 2012139, the National Science Foundation under Grant Nos. CCF-1329374, CCF-1526466, and CNS-1548078, IARPA under Grant No. W911NF-14-C-0089, and by grants from Cisco Systems and Intel.

IoT devices are typically intended to be self powered. Some low cost and easily accessible devices can be replaced when the battery becomes depleted; however, other devices are dependent on alternative forms of energy to prolong lifetime. Four basic forms of energy exist in the ambient [4], (1) electromagnetic (EM), (2) solar, (3) thermal, and (4) kinetic. The most common energy harvesting circuits target solar and electromagnetic energy. It has been experimentally shown that the ambient exhibits EM power densities of 0.1 to 1 μW/cm^2 [5]. The available solar power density in the ambient is on the order of mW when illuminated using the standard global solar irradiance spectrum [6]. The magnitude of the harvested thermal power, using a thermoelectric generator (TEG), and kinetic power, using a piezoelectric device is, respectively, 0.52 mW and 8.4 mW [4]. The different types of energy in the ambient and the range of harvested power are summarized in Table I.

Hybrid energy harvesting circuits have recently been developed for solar and EM energy [7]. The 3-D platform, however, can integrate the available energy harvesting methods within a single structure. In addition to harvesting multiple sources of energy (solar, EM, thermal, and kinetic, see Figure 1), the power efficiency of delivering harvested power to the load in 3-D ICs is higher than in conventional two-dimensional (2-D) ICs. Each energy harvesting circuit benefits from different substrate materials. For example, efficient solar cells have been demonstrated on a PET substrate [8], while thermoelectric circuits are commercially available using a Bi_2Te_3 substrate [9]. The 3-D platform supports the integration of these heterogeneous substrates within a single, small platform.

Communication circuits typically consume significant power to transmit data. The power overhead occurs when initializing the transmitter. To lower this power overhead, memory arrays are sometimes included within the IoT devices. The data are stored in memory and transmitted at a later time when a sufficient amount of data has been accumulated. Advanced memory technologies can also be seamlessly integrated

TABLE I
Typical harvested power for different energy types available from the ambient [4]–[6]

Energy type	Harvested power
EM	0.1 to 1 μWatt
Solar	1 to 10 mWatt
Thermal	0.52 mWatt
Kinetic	8.4 mWatt

978-1-4673-6853-7/17/$31.00 ©2017 IEEE

TABLE II

COMMON CIRCUITS AND COMPATIBLE SUBSTRATE TYPES

Applications	Substrate materials	Electrical resistivity $\Omega \cdot$ cm	Thermal conductivity W/(m°K)	Refractive index	Young's modulus GPa	Thermal expansion coefficient at 300°K 10^{-6}/°K	Wavelength range nm
Processor/ memory	Silicon (Si)	1 to 10	138	3.4 to 3.5	130 to 185	2.6	400 to 1,060
Solar cells	Polyethylene Terephthalate (PET)	$1 \cdot 10^{16}$	0.2	1.6	2 to 2.7	3.9	400 to 1,600
Thermoelectric	Bismuth Telluride (Bi_2Te_3)	$0.6 \cdot 10^{-3}$	1.2	9.2	50 to 55	1.3	400 to 2,500
Piezoelectric	Aluminum Nitride (AlN)	$1 \cdot 10^{14}$	140 to 180	1.9 to 2.2	308	5.27	1,000 to 1,500
RF/analog	Gallium Arsenide (GaAs)	$4 \cdot 10^{7}$	40	3.9	85.9	6.86	650 to 870
Photonics	Germanium (Ge)	$1 \cdot 10^{-3}$	45	4 to 4.1	102.7	5.8	600 to 1,600
Space/ detectors	Mercury Cadmium Telluride (HgCdTe)	2	0.2	4	42 to 48	4.7	2,000 to 5,400

within a 3-D IC, exploiting ferromagnetic substrate materials and the short distance to the computational layer.

The rest of the paper is composed of the following sections. Common IoT circuits and substrate materials are reviewed in Section II. A hybrid energy harvesting system within a 3-D platform is described in Section III. The efficiency of the hybrid system is discussed in Section IV. Some conclusions are offered in Section V.

II. COMMON IOT CIRCUITS AND SUBSTRATE TYPES

Each layer in a 3-D IC is individually fabricated using a process optimized for that application [2]. Different substrate materials are compatible with different circuits. The electrical, thermal, mechanical, and optical properties of certain substrate materials used in common ICs for IoT devices are listed in Table II.

Each of the substrate materials listed in Table II is beneficial for a certain type of circuit. Silicon (Si) is typically lower cost and technologically more mature than the other materials listed in Table II, and is therefore used for mainstream, high complexity processor and memory applications. Polyethylene terephthalate (PET) is low cost and provides high transparency [8]. PET is used as the substrate of p-i-n type solar cells and is compatible with traditional deposition processes of solar cells on glass substrates [8]. Thermoelectric generators (TEG) typically consist of multiple pairs of p-type and n-type bismuth telluride (Bi_2Te_3) thermoelectric structures, which produce electrical energy by exploiting temperature gradients between the hot surface (human body) and the cold surface (ambient air) [9], [10]. Aluminum nitride (AlN) is commonly used for piezoelectric devices as this material can be processed by CMOS compatible technologies at low temperature (200°C to 400°C). AlN also exhibits higher phase velocity and a moderately high piezoelectric coefficient than other piezoelectric materials (*e.g.*, GaN and ZnO) [11]. Piezoelectric sensors can harvest kinetic energy from the ambient. This energy originates from vibrations and other physical movement. Piezoelectric sensors capture and transform these motions into electrical energy. The superior electron mobility and direct bandgap of gallium arsenide (GaAs) makes GaAs attractive for certain high performance digital, analog, and optical applications. Germanium (Ge) is also a favorable substrate material for photovoltaic and photodetector systems due to the high absorption coefficient of Ge. Military and space application that require high quality infrared detectors commonly use mercury cadmium telluride (HgCdTe) which has a tunable bandgap ranging from 0.1 eV to 1 eV [12]. This property of HgCdTe supports detection of long wavelengths of light. Each of these technologies can support a variety of IoT applications while comfortably fitting into a single 3-D system.

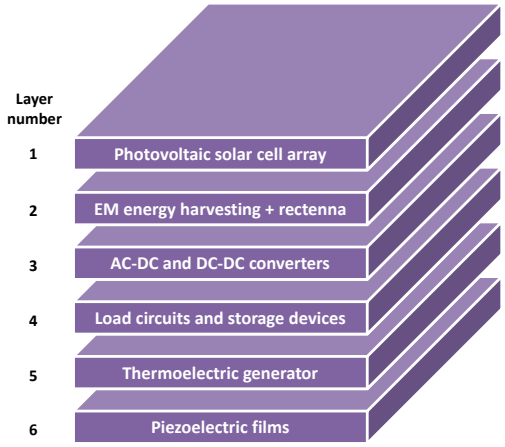

Fig. 1. Proposed hybrid harvesting 3-D system.

III. HYBRID HARVESTING SYSTEM WITHIN A 3-D PLATFORM

The topology of the proposed hybrid energy harvesting system within a 3-D platform is shown in Figure 1. Each layer of the 3-D IC consists of an individual substrate material, fabricated using a process optimized for that technology. The layers are interconnected using TSVs to create short low impedance interconnections between the layers. Low power dissipation is a key objective for IoT devices, therefore, utilizing a 3-D structure, as illustrated in Figure 1, with short vertical interconnections is highly desirable.

The proposed system consists of energy harvesting mechanisms for each type of ambient energy. For solar energy harvesting, on-chip solar cells (*e.g.*, photodiodes) are integrated on layer 1. The harvested DC power is directed to the conversion layer (layer 3) using TSVs. Two sets of stacked

TSVs deliver power to the conversion layer with a total vertical interconnect length of ∼ 40 μm. For EM energy harvesting, an on-chip rectifying antenna (rectenna) is placed on layer 2 of the hybrid 3-D system. The harvested DC power is transferred using TSVs on layer 3 and, if necessary, converted to a different voltage level. A TEG is placed on layer 5 of the harvesting system (see Figure 1). The TEG is an on-chip DC voltage source [13]; power conversion is therefore not required. The TEG-based voltage sources supply current to the load circuits on layer 4 of the proposed system. Piezoelectric films are deposited on layer 6 of the hybrid harvesting structure. AC power is delivered to layer 3 and converted to DC using AC-to-DC converters placed on this layer.

On-chip converters [14] are utilized within the conversion system on layer 3 of the 3-D system. These converters typically exhibit a high conversion efficiency (above 99%) due to reduced parasitic impedances. Integrating the harvesting mechanisms (solar cells, rectenna, TEG, piezoelectric films) onto a 3-D platform increases the efficiency of the overall system by reducing the parasitic impedances.

The energy available from the ambient is typically scarce, therefore integrating harvesting circuits that exploit multiple types of energy sources within a single system is an effective approach. In the hybrid system, power is simultaneously harvested from the different sources depending upon the availability of each type of energy. Since the availability of the different energies is inconsistent (*e.g.*, no solar energy during cloudy days or at night, or no kinetic energy when stationary), certain harvesting systems may be turned off (sleep mode) while other systems continue to harvest available energy. This feature reduces leakage power in non-utilized systems while harvesting power from available forms of energy.

An electrical model of the proposed hybrid harvesting system within a 3-D platform is shown in Figure 2. TSVs transfer power between the layers of the 3-D IC, and are modeled as resistors with a coupling capacitor to the substrate. Different models for each type of substrate are applicable [3].

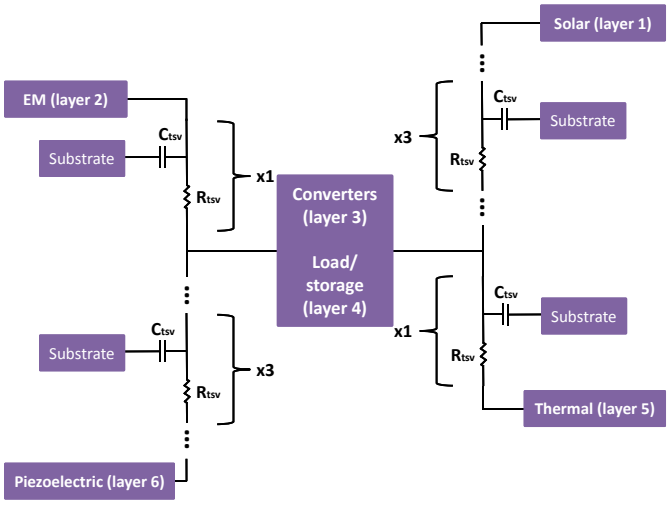

Fig. 2. Model of TSV impedances within proposed 3-D hybrid harvesting system.

In addition, depending upon the resistivity of the substrate, a distributed model may be required rather than a lumped model, as shown in Figure 2.

IV. Efficiency of Hybrid Harvesting System

An energy harvesting system is shown in Figure 3. The power harvested from the ambient P_h is strongly dependent upon the type of harvested energy and harvesting mechanism. The harvested power is converted and delivered to either the load or on-chip capacitive storage devices (*e.g.*, micro supercapacitors [15]). In certain harvesting mechanisms, as described in Section III, only DC-DC conversion or no conversion is required.

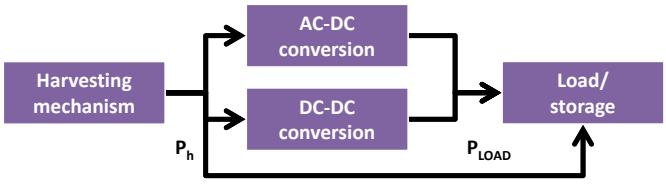

Fig. 3. Energy harvesting system.

The power efficiency and output voltage levels of each on-chip harvesting system are summarized in Table III. Piezoelectric films and solar cells exhibit high harvesting efficiencies, respectively, 91% and 59% [16], [17]. The high harvesting efficiency combined with the available ambient power (see Table I) makes these two sources of energy highly desirable. Piezoelectric energy is also typically scarce when stationary since vibrations are required by the piezoelectric harvesting system. Alternatively, EM and thermal energy are typically always available although at significantly lower levels. The harvesting efficiency of on-chip rectennas and TEG device is low, respectively, 2% and 0.15% [18], [19]. Power delivery techniques are required to combine the harvested energy and distribute the multiple generated voltages across a 3-D IC.

The total power delivered to the load using these hybrid harvesting systems is

$$P_{\text{delivered}}^{\text{total}} = P_{\text{delivered}}^{\text{EM}} + P_{\text{delivered}}^{\text{solar}} + P_{\text{delivered}}^{\text{thermal}} + P_{\text{delivered}}^{\text{piezo}} \quad , \quad (1)$$

where $P_{\text{delivered}}^{\text{total}}$ is the total power delivered to the load and is the sum of the power harvested by each type of harvesting mechanism. Each harvesting system delivers power according to

$$P_{\text{delivered}} = \alpha P_{\text{ambient}} \cdot \eta \quad , \quad (2)$$

where η is the efficiency of the specific harvesting system, and α is the availability of the specific energy within the ambient,

TABLE III
Experimental efficiency and output voltage of on-chip harvesting systems

Harvester type	Efficiency	Output voltage [V]	References
Rectenna	2%	< 3.1	[18]
Solar cells	59%	1.3 to 2.8	[17]
TEG	0.15%	< 1.5	[19]
Piezoelectric film	91%	0.5 to 3.2	[16]

ranging from 0 to 1. The following values for α are assumed here: $\alpha^{\text{EM}} = 1$, $\alpha^{\text{solar}} = 0.3$, $\alpha^{\text{thermal}} = 0.8$, and $\alpha^{\text{piezo}} = 0.05$. Applying (2) with the power harvesting efficiencies listed in Table III and the average ambient power (see Table I), the delivered power for each type of ambient energy is

$$P^{\text{EM}}_{\text{delivered}} = \alpha^{\text{EM}} \cdot P^{\text{EM}}_{\text{harvested}} \cdot \eta^{\text{EM}} = 1 \cdot 0.55\ \mu\text{W} \cdot 0.02 = 0.011\ \mu\text{W} \quad (3)$$

$$P^{\text{solar}}_{\text{delivered}} = \alpha^{\text{solar}} \cdot P^{\text{solar}}_{\text{harvested}} \cdot \eta^{\text{solar}} = 0.3 \cdot 5.5\ \text{mW} \cdot 0.59 = 0.97\ \text{mW} \quad (4)$$

$$P^{\text{thermal}}_{\text{delivered}} = \alpha^{\text{thermal}} \cdot P^{\text{thermal}}_{\text{harvested}} \cdot \eta^{\text{themal}} = 0.8 \cdot 0.52\ \text{mW} \cdot 0.15 = 0.062\ \text{mW} \quad (5)$$

$$P^{\text{piezo}}_{\text{delivered}} = \alpha^{\text{piezo}} \cdot P^{\text{piezo}}_{\text{harvested}} \cdot \eta^{\text{piezo}} = 0.05 \cdot 8.4\ \text{mW} \cdot 0.91 = 0.38\ \text{mW} \quad (6)$$

resulting in a total delivered power,

$$P^{\text{total}}_{\text{delivered}} = 0.011\ \mu\text{W} + 0.97\ \text{mW} + 0.062\ \text{mW} + 0.38\ \text{mW} = 1.41\ \text{mW}\ . \quad (7)$$

Assuming an ultra-low power supply voltage V_{DD} = 0.5 volts and a maximum load current I_{max} = 1.6 mA required for sensing, computation, and communication of a typical IoT device [20], the maximum required power is

$$P_{\text{required}} = V_{DD} \cdot I_{max} = 0.5\ \text{V} \cdot 1.6\ \text{mA} = 0.8\ \text{mW}\ , \quad (8)$$

less than 57% of the available power.

The energy efficiencies listed in Table III are based on experimentally evaluated systems [16]–[19] developed within classical 2-D ICs. These systems include off-chip components. A large form factor and multi-millimeter interconnects are required to integrate multiple harvesting circuits within a single 2-D IC. These issues render a 2-D IC approach significantly less effective than a 3-D platform for IoT devices.

V. Conclusions

3-D ICs are a natural platform for IoT devices. The 3-D structure provides opportunities to enhance the internal power and external communication of IoT devices. 3-D ICs provide a platform for heterogeneous integration of the disparate technologies required for IoT systems, including different substrate materials and unique processing of individual layers. The 3-D platform also provides the small form factor necessary for small IoT devices. In addition, improved power efficiency is exhibited due to lower parasitic interconnect impedances.

Hybrid power harvesting of all four energy forms available in the ambient is supported by the 3-D structure, leading to self sustainable, miniature, and intelligent systems. The different harvesting circuits can be integrated onto different layers within a 3-D structure. The harvested power is transferred using TSVs to the load and storage circuits, or to a separate layer where AC-to-DC or DC-to-DC conversion is performed. The benefit of a hybrid harvesting system is the increased energy available from individually scarce and inconsistent sources of energy. A 3-D IC-based hybrid harvesting system is shown to be capable of supplying the required power to IoT devices.

References

[1] D. Blaauw, D. Sylvester, P. Dutta, Y. Lee, I. Lee, S. Bang, Y. Kim, G. Kim, P. Pannuto, Y. S. Kuo, D. Yoon, W. Jung, Z. Foo, Y. P. Chen, S. Oh, S. Jeong, and M. Choi, "IoT Design Space Challenges: Circuits and Systems," *Proceedings of the IEEE Symposium on VLSI Technology*, pp. 1 – 2, June 2014.

[2] V. F. Pavlidis and E. G. Friedman, *Three-Dimensional Integrated Circuit Design*, Morgan Kaufmann, 2009.

[3] B. Vaisband and E. G. Friedman, "Noise Coupling Models in Heterogeneous 3-D ICs," *IEEE Transactions on Very Large Scale Integration (VLSI) Systems*, Vol. 24, No. 8, pp. 2778 – 2786, August 2016.

[4] A. Georgiadis, "Energy Harvesting for Autonomous Wireless Sensors and RFID's," *Proceedings of the IEEE General Assembly and Scientific Symposium*, pp. 1 – 5, August 2014.

[5] H. J. Visser, A. C. F. Reniers, and J. A. C. Theeuwes, "Ambient RF Energy Scavenging: GSM and WLAN Power Density Measurements," *Proceedings of the IEEE European Microwave Conference*, pp. 721 – 724, October 2008.

[6] D. G. Collins, W. G. Blattner, M. B. Wells, and H. G. Horak, "Backward Monte Carlo Calculations of Polarization Characteristics of the Radiation Emerging from Spherical Shell Atmospheres," *Applied Optics*, Vol. 11, No. 11, pp. 2684 – 2696, November 1972.

[7] I. J. Hwang, D. Kwon, D. J. Lee, J. W. Yu, and W. S. Lee, "EM/light Hybrid Energy Harvesting with Directional Dipole Antenna for IoT Sensor," *Proceedings of the IEEE Antennas and Propagation Society International Symposium*, pp. 1292 – 1293, July 2015.

[8] J. Ni, J. Zhang, J. Xue, X. Wang, L. Cao, C. Wu, S. Xiong, X. Geng, and Y. Zhao, "Effect of Pretreatment on PET Films and its Application for Flexible Amorphous Silicon Solar Cells," *Proceedings of the IEEE Photovoltaic Specialists Conference*, pp. 293 – 296, June 2009.

[9] Micropelt, "Thermogenerators," 2016. [Online]. Available: http://www.micropelt.com/thermogenerator.php.

[10] C. Lu, S. P. Park, V. Raghunathan, and K. Roy, "Efficient Power Conversion for Ultra Low Voltage Micro Scale Energy Transducers," *Proceedings of the IEEE Design, Automation, and Test Conference in Europe*, pp. 1602 – 1607, March 2010.

[11] K. Wasa, T. Matsushima, H. Adachi, I. Kanno, and H. Kotera, "Thin-Film Piezoelectric Materials for a Better Energy Harvesting MEMS," *Journal of Microelectromechanical Systems*, Vol. 21, No. 2, pp. 451 – 457, April 2012.

[12] A. L. Betz and R. T. Boreiko, "Space Applications for HgCdTe at FIR Wavelengths between 50 and 150 um," *Proceedings of the SPIE Materials for Infrared Detectors*, pp. 1 – 9, November 2001.

[13] R. Buzilo, B. Likhterov, R. Giterman, I. Levi, A. Fish, and A. Belenky, "Approach to Integrated Energy Harvesting Voltage Source Based on Novel Active TEG Array System," *Proceedings of the IEEE Faible Tension Faible Consommation*, pp. 1 – 4, May 2014.

[14] I. Vaisband, M. Saadat, and B. Murmann, "A Closed-Loop Reconfigurable Switched-Capacitor DC-DC Converter for Sub-mW Energy Harvesting Applications," *IEEE Transactions on Circuits and Systems I: Regular Papers*, Vol. 62, No. 2, pp. 385 – 394, February 2015.

[15] B. Song, K. S. Moon, and C. P. Wong, "Recent Developments in Design and Fabrication of Graphene-Based Interdigital Micro-Supercapacitors for Miniaturized Energy Storage Devices," *IEEE Transactions on Components, Packaging and Manufacturing Technology*, 2016, in press.

[16] X. D. Do, H. H. Nguyen, S. K. Han, D. S. Ha, and S. G. Lee, "A Self-Powered High-Efficiency Rectifier With Automatic Resetting of Transducer Capacitance in Piezoelectric Energy Harvesting Systems," *IEEE Transactions on Very Large Scale Integration (VLSI) Systems*, Vol. 23, No. 3, pp. 444 – 453, March 2015.

[17] S. Ghosh, H. T. Wang, and W. D. Leon-Salas, "A Circuit for Energy Harvesting Using On-Chip Solar Cells," *IEEE Transactions on Power Electronics*, Vol. 29, No. 9, pp. 4658 – 4671, September 2014.

[18] N. Weissman, S. Jameson, and E. Socher, "W-Band CMOS On-Chip Energy Harvester and Rectenna," *Proceedings of the IEEE International Microwave Symposium*, pp. 1 – 3, June 2014.

[19] K. Y. Lee, D. Brown, and S. Kumar, "Silicon Nanowire Arrays Based On-Chip Thermoelectric Generators," *IEEE Transactions on Components, Packaging and Manufacturing Technology*, Vol. 5, No. 8, pp. 1100 – 1107, August 2015.

[20] B. Martinez, M. Montón, I. Vilajosana, and J. D. Prades, "The Power of Models: Modeling Power Consumption for IoT Devices," *IEEE Sensors Journal*, Vol. 15, No. 10, pp. 577 – 5789, October 2015.